Energy & Environmental Science

COMMUNICATION

View Article Online
View Journal | View Issue

Cite this: *Energy Environ. Sci.*, 2015, **8**, 203

Received 22nd September 2014
Accepted 29th October 2014

DOI: 10.1039/c4ee03012e

www.rsc.org/ees

Stabilization of Si microwire arrays for solar-driven H_2O oxidation to O_2(g) in 1.0 M KOH(aq) using conformal coatings of amorphous TiO_2†

Matthew R. Shaner,[ab] Shu Hu,[ab] Ke Sun[ab] and Nathan S. Lewis*[abcd]

Conductive, amorphous TiO_2 coatings deposited by atomic-layer deposition, in combination with a sputter deposited $NiCrO_x$ oxygen-evolution catalyst, have been used to protect Si microwire arrays from passivation or corrosion in contact with aqueous electrolytes. Coated np^+-Si/TiO_2/$NiCrO_x$ as well as heterojunction n-Si/TiO_2/$NiCrO_x$ Si microwire-array photoanodes exhibited stable photoelectrochemical operation in aqueous ferri-/ferro-cyanide solutions. The coatings also allowed for photoanodic water oxidation in 1.0 M KOH(aq) solutions for >2200 h of continuous operation under simulated 1 Sun conditions with ~100% Faradaic efficiency for the evolution of O_2(g).

Broader context

Photoelectrochemical conversion of sunlight into hydrogen has the ability to provide continuous, carbon-free energy, but in order to be an economically competitive energy source the system must be both efficient and stable for years of operation. This combination proves challenging as the most efficient semiconductors for solar-energy conversion are unstable after only seconds to minutes of operation, especially under oxidizing conditions. Accordingly, improving the stability while maintaining efficient operation is an important goal in furthering this technology and is the subject herein as demonstrated by a two-step approach. First, increasing the electrochemically active *versus* geometrical surface area with a periodically structured Si microwire array decreases the effective current density at the solid/solution interface and thus the rate of corrosion. Secondly, a conformal, transparent, electrically conductive protection layer serves as a corrosion-resistant barrier between the semiconductor and solution while maintaining efficient charge transfer to the reaction site.

Technologically important, small band-gap semiconductors such as Si are highly attractive materials for use as photoanodes to oxidize water, but are unstable to corrosion and/or passivation under anodic conditions in aqueous electrolytes.[1] Single crystalline n-Si, n-GaAs, n-GaP, n-CdTe, and n-$BiVO_4$ photoanodes have all recently demonstrated enhanced stability (4–100+ hours) under continuous operation for water oxidation to O_2(g) in aqueous alkaline electrolytes, with 100% Faradaic efficiency, by use of electrically conductive, optically transparent, 10–100 nm thick protective films of amorphous TiO_2 deposited by atomic-layer deposition (ALD).[2–4] Arrays of semiconductor microwires or nanowires provide an especially attractive system architecture for the direct production of fuels from sunlight, because such a structure provides a minimal path for ionic conduction, high optical absorption,[5–9] a high surface-area support for electrocatalyst loading,[10] and other distinctive, advantageous operational features.[11] The application of conformal protective films to such highly anisotropic structures by use of sputtering or evaporation is expected to be difficult, whereas the self-limiting ALD surface condensation reaction technique is a conformal coating process. Accordingly, we describe herein the use of ALD-deposited amorphous TiO_2 films to enable the continuous oxidation of water to O_2(g) by Si microwire array photoanodes for >2200 h in 1.0 M KOH(aq) under simulated 1 Sun illumination conditions.

To fabricate the structures of interest, arrays of n-type and np^+-radial junction Si microwires were coated with ALD-grown TiO_2,[4] followed by deposition of a nickel–chromium oxide oxygen-evolution catalyst using magnetron sputtering (see the ESI† for full Experimental details). Fig. 1a shows a schematic of the process, and Fig. 1b and c show scanning-electron micrographs (SEM) of the Si microwire arrays before and after deposition of the TiO_2 protective coating (2000 ALD cycles, ~94 nm) and the $NiCrO_x$ catalyst layer (20 min sputtering, ~40 nm planar equivalent), respectively. Fig. 1d shows a cross-section near the base of a single fully processed (np^+-Si/TiO_2/$NiCrO_x$) microwire within an array, demonstrating that the fabrication produced the desired structure as well as a conformal layer of TiO_2 having

[a]*Division of Chemistry and Chemical Engineering, California Institute of Technology, Pasadena, CA 91125, USA. E-mail: nslewis@caltech.edu*

[b]*Joint Center for Artificial Photosynthesis, California Institute of Technology, Pasadena, CA 91125, USA*

[c]*Beckman Institute Molecular Materials Research Center, California Institute of Technology, Pasadena, CA 91125, USA*

[d]*Kavli Nanoscience Institute, California Institute of Technology, Pasadena, CA 91125, USA*

† Electronic supplementary information (ESI) available: Experimental methods and supplementary data. See DOI: 10.1039/c4ee03012e

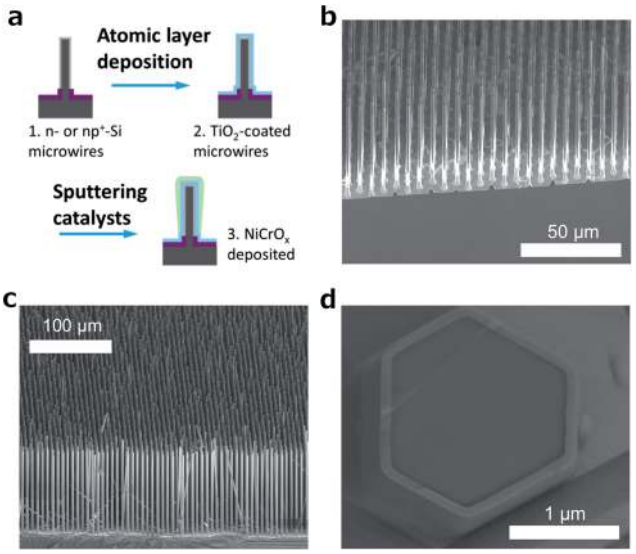

Fig. 1 (a) Schematic of a structure that consists of an np^+-Si microwire-array conformally coated with a protective, transparent and hole-conducting TiO_2 layer, with the TiO_2 layer subsequently coated with a $NiCrO_x$ oxygen-evolution catalyst. (b) Scanning-electron micrograph (SEM) images of an np^+-Si microwire-array prior to further processing. (c) SEM image of a fully processed microwire array. (d) SEM cross-section near the base of a single microwire, showing the conformality of the TiO_2 coating with a thickness of 94 nm.

a relatively uniform thickness along the height of the wire. A detailed inspection of an individual Si microwire indicated that the $NiCrO_x$ deposited at the top and base of each Si microwire, due to the relatively line-of-sight deposition profile of the magnetron sputtering process. Only the regions of the $NiCrO_x$ catalyst on the surfaces of the wires are expected to be electrocatalytically active, due to the electrically insulating SiO_2 on the sample substrate.

Fig. 2 shows the current density *vs.* potential (*J–E*) behavior of an np^+-Si/TiO_2/$NiCrO_x$ microwire-array photoelectrode in contact with (a) 1.0 M KOH(aq) (pH = 13.6) and (b) 0.50 M K_2SO_4–0.050 M $K_3Fe(CN)_6$–0.35 M $K_4Fe(CN)_6$(aq) in the presence and absence, respectively, of 100 mW cm^{-2} of simulated Air Mass (AM) 1.5G illumination. Fig. 2a also depicts the *J–E* behavior of a p^+-Si/TiO_2/$NiCrO_x$ microwire-array electrode in the absence of illumination, to allow for a comparison of the onset potentials for the oxygen-evolution reaction between the illuminated photoanode and a degenerately doped unilluminated p^+-Si anode. The one-electron, outer-sphere, reversible $Fe(CN)_6^{3-/4-}$ redox couple was used to measure the intrinsic energy-conversion properties of the microwire-array photoanodes. Under 100 mW cm^{-2} of simulated Air Mass (AM) 1.5G illumination, the np^+-Si/TiO_2/$NiCrO_x$ microwire array produced an open-circuit potential (E_{oc}) of −0.62 V *vs.* the formal potential for water oxidation, $E^{0'}(O_2/OH^-)$, and a light-limited photocurrent density (J_{ph}) of 7.1 mA cm^{-2} in 1.0 M KOH(aq), and produced E_{oc} = −0.44 V *vs.* the Nernstian potential of the solution ($E(Fe(CN)_6^{3-/4-})$) and J_{ph} = 7.3 mA cm^{-2} in contact with $Fe(CN)^{3-/4-}$(aq). A diode quality factor of 1.9–2.2 was measured in contact with $Fe(CN)^{3-/4-}$(aq) from the *J–E* data obtained as a function of illumination intensity.[5,12] The intrinsic photoelectrode behavior observed for the np^+-Si/TiO_2/$NiCrO_x$ photoanode in contact with the one-electron, reversible, $Fe(CN)_6^{3-/4-}$ redox system (Fig. 2b) demonstrated an energy-conversion efficiency of 1.8% with a fill factor of 0.54.

For comparison, Fig. 3 shows the *J–E* behavior in the presence and absence of illumination, respectively, of n-Si/TiO_2/$NiCrO_x$ microwire-array photoelectrodes in (a) 1.0 M KOH and (b) an aqueous $Fe(CN)_6^{3-/4-}$ solution. In contact with 1.0 M KOH(aq), these samples exhibited E_{oc} = −0.49 V *vs.* $E^{0'}(O_2/OH^-)$ and J_{ph} = 3.7 mA cm^{-2} (Fig. 3a), whereas in contact with $Fe(CN)_6^{3-/4-}$(aq) the n-Si/TiO_2/$NiCrO_x$ microwire arrays exhibited E_{oc} = −0.18 V *vs.* $E(Fe(CN)_6^{3-/4-})$ and J_{ph} = 3.1 mA cm^{-2}. The intrinsic photoelectrode behavior observed for the n-Si/TiO_2/$NiCrO_x$ photoanode in contact with the $Fe(CN)_6^{3-/4-}$ redox system (Fig. 2b) demonstrated an energy-conversion efficiency of 0.3% with a fill factor of 0.51. When measured under nominally identical conditions, all (6 electrodes) of the microwire-array photoelectrodes studied herein showed mutually similar photovoltages, but exhibited variable photocurrent densities with a spread of ~5 mA cm^{-2}, consistent with a variation in wire height at various locations on the wafer from which the

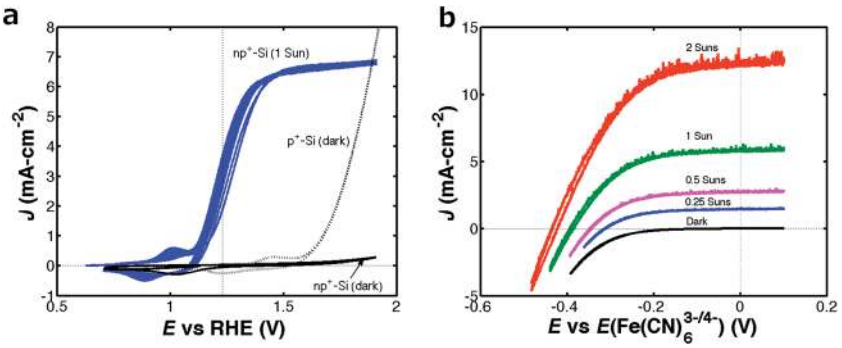

Fig. 2 Current density *versus* potential performance of np^+-Si/TiO_2/$NiCrO_x$ microwire-array photoelectrodes in contact with (a) 1.0 M KOH(aq) and (b) $Fe(CN)_6^{3-/4-}$(aq). (a) The solid blue curve is under 1-Sun simulated illumination, the solid black curve is under no illumination, dark, and the dashed black curve is the performance of a p^+-Si/TiO_2/$NiCrO_x$ microwire-array electrode. The potential is plotted versus the potential of the reversible hydrogen electrode (RHE). The illumination intensity in (b) was adjusted using a series of 0.3 optical density neutral-density filters, with the illumination intensity labeled on the plot.

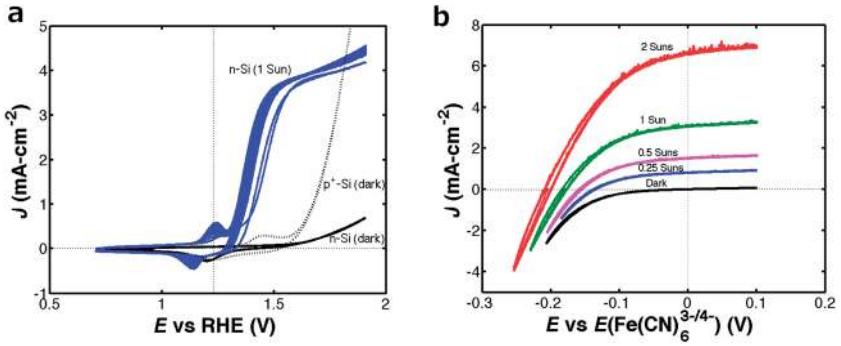

Fig. 3 Current density *versus* potential data for n-Si/TiO_2/$NiCrO_x$ microwire-array photoelectrodes in contact with (a) 1.0 M KOH(aq) and (b) $Fe(CN)_6^{3-/4-}$(aq). (a) The solid blue curve is under 1 Sun simulated illumination, the solid black curve is in the absence of illumination, dark, and the dashed black curve is the performance of a p^+-Si/TiO_2/$NiCrO_x$ microwire-array electrode. (b) The illumination intensity was adjusted using a series of 0.3 optical density neutral-density filters, with the resulting illumination intensity labeled on the plot.

electrodes were fabricated.[13,14] The addition of scattering particles can significantly increase J_{ph} by increasing the illumination path length through the photoactive Si microwire array.[15]

Fig. 4a shows the external quantum yield (Φ_{ext}) for np^+-Si/TiO_2/$NiCrO_x$ and n-Si/TiO_2/$NiCrO_x$ microwire-array photoelectrodes in contact with 1.0 M KOH(aq). The observed behavior was similar to that obtained previously for microwire-array photocathodes and photovoltaics illuminated at normal incidence.[15] The Φ_{ext} exhibited a similar dependence on wavelength for both the np^+-Si and the n-Si microwire arrays, consistent with behavior dominated by absorption and charge-carrier collection in a microwire array. Integration of the wavelength-dependent spectral response data of protected np^+-Si and n-Si microwire-arrays with respect to the AM 1.5G solar spectrum yielded calculated photocurrent densities of 7.9 mA cm^{-2} and 2.9 mA cm^{-2}, respectively, in excellent agreement with the J_{ph} values measured from the *J–E* behavior.

Fig. 5a shows the time dependence of the photocurrent density of an np^+-Si microwire array under potentiostatic control at 0.36 V *vs.* $E^{0'}(O_2/OH^-)$ (0.70 V *vs.* a Hg/HgO reference electrode). Fig. 5b shows the *J–E* data at 10 h intervals throughout the stability test, showing no significant change in

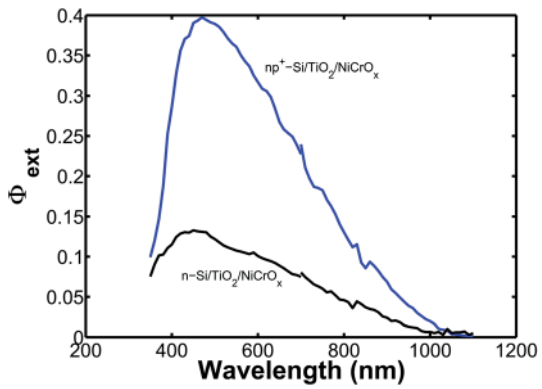

Fig. 4 External quantum yield (Φ_{ext}) *versus* wavelength plot of representative protected n-Si and np^+-Si microwire-array photoelectrodes in contact with 1.0 M KOH(aq).

J_{ph}, E_{oc} or fill factor during the stability evaluation. As shown in Fig. 5c, a comparison between the amount of O_2(g) expected based on Coulomb's law and the amount of O_2(g) detected using a calibrated fluorescent O_2(g) probe indicated ~100% Faradaic efficiency for oxygen evolution. Assuming four electrons per Si atom dissolved, the total number of coulombs of charged passed during the stability test, 6000 C, exceeded by a factor of 20 the 300 C of charge that would have been required to dissolve the entire Si microwire array. Furthermore, assuming that 10 nm of oxide formation would result in complete passivation of the electrode, the amount of charge passed establishes a lower limit of 9×10^4 on the branching ratio for water oxidation to O_2(g) relative to oxidation of the Si.

Accounting for the ~20% capacity factor of sunlight, the 2200 h of continuous operation contained the same amount of charge as would be passed during >1 year of outdoor operation. Because lower current densities away from peak illumination times of day would likely increase the stability, this projected >1 year stability plausibly represents a lower limit on the actual stability of the NiO_x-coated Si photoanodes under operational conditions. A detailed failure analysis study and validated accelerated testing protocols, additionally incorporating possible effects of temperature cycling and extended periods of no photocurrent current due to day/night cycling, would clearly be required to establish the ultimate limit on the stability of the photoanodes described herein. The high internal surface area of a highly anisotropic structure such as a microwire array produces a correspondingly low current density at the areas exposed to the electrolyte. This low current density is expected to beneficially reduce the rate of light-intensity-dependent photocorrosion or photopassivation processes, because the photon flux per projected geometric area provided by sunlight produces minority-carrier currents that are distributed over a large internal surface area of the solid/liquid contact in the internal volume of a microwire array. Consistently, the microwire arrays exhibited a greater degree of stability than crystalline Si electrodes protected by amorphous TiO_2 films and operated at 30 mA cm^{-2}, which exhibited a small but significant decay in photocurrent after 24 h of continuous operation in the same electrolyte.[4]

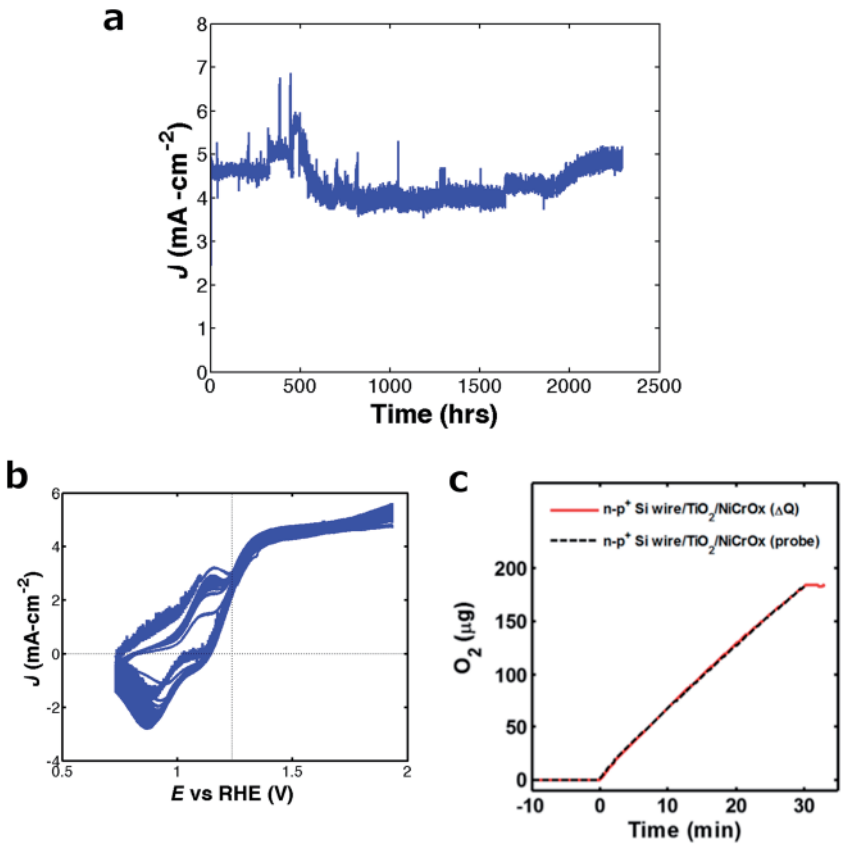

Fig. 5 (a) Current density *versus* time for an n-p^+-Si/TiO_2/$NiCrO_x$ microwire-array photoelectrode under 1 Sun simulated illumination in 1.0 M KOH(aq) under potential control at 0.36 V *vs.* $E^{0'}(OH^-/O_2)$. (b) Current density *versus* potential behavior of cyclic voltammograms taken at 10 h intervals throughout the duration of the stability test. (c) Oxygen production as a function of time in 1.0 M KOH(aq) while under potential control at 0.36 V *vs.* $E^{0'}(OH^-/O_2)$. The Faradaic efficiency for oxygen evolution, ~100%, was determined by comparing the observed oxygen produced relative to the amount expected based on the total current passed in conjunction with the use of Faraday's law.

Incorporation of the np$^+$-Si/TiO_2/$NiCrO_x$ photoanode into a complete water-splitting device operating at 10% solar-to-hydrogen efficiency would require a photocathode capable of producing >10 mA cm^{-2} at 1.5 V and addition of scattering particles to increase the absorption and current density in the Si microwires.[15] For efficient operation, such a photocathode, operating near its Shockley–Quiesser limit, would need to have a band gap of ~2.0 eV with either a buried junction or proper band positioning relative to the hydrogen-evolution potential. The observations reported herein therefore illustrate an additional advantage of the amorphous TiO_2-based protection strategy in that the deposition method, ALD, is especially well suited to be compatible with a wide range of high-efficiency materials while also being compatible with a broad range of morphologies associated with highly anisotropic structures of the light absorber.

Acknowledgements

The authors would like to acknowledge Dr Ragip Pala for assistance with the spectral response measurement system. This material is based upon work performed by the Joint Center for Artificial Photosynthesis, a DOE Energy Innovation Hub, supported through the Office of Science of the U.S. Department of Energy under Award Number DE-SC0004993. M. R. S. is supported by a graduate fellowship from the Resnick Institute for Sustainability. The authors also acknowledge support from the Gordon and Betty Moore Foundation.

Notes and references

1 J. R. McKone, N. S. Lewis and H. B. Gray, *Chem. Mater.*, 2014, **26**, 407–414.
2 M. F. Lichterman, A. I. Carim, M. T. McDowell, S. Hu, H. B. Gray, B. S. Brunschwig and N. S. Lewis, *Energy Environ. Sci.*, 2014, **7**, 3334–3337.
3 M. T. McDowell, M. F. Lichterman, J. M. Spurgeon, S. Hu, I. D. Sharp, B. S. Brunschwig and N. S. Lewis, *J. Phys. Chem. C*, 2014, **118**, 19618–19624.
4 S. Hu, M. R. Shaner, J. A. Beardslee, M. Lichterman, B. S. Brunschwig and N. S. Lewis, *Science*, 2014, **344**, 1005–1009.
5 S. Hu, C.-Y. Chi, K. T. Fountaine, M. Yao, H. A. Atwater, P. D. Dapkus, N. S. Lewis and C. Zhou, *Energy Environ. Sci.*, 2013, **6**, 1879.

6 A. R. Madaria, M. Yao, C. Chi, N. Huang, C. Lin, R. Li, M. L. Povinelli, P. D. Dapkus and C. Zhou, *Nano Lett.*, 2012, **12**, 2839–2845.
7 J. Zhu, Z. Yu, G. F. Burkhard, C.-M. Hsu, S. T. Connor, Y. Xu, Q. Wang, M. McGehee, S. Fan and Y. Cui, *Nano Lett.*, 2009, **9**, 279–282.
8 A. Chutinan and S. John, *Phys. Rev. A*, 2008, **78**, 023825.
9 T. Tayagaki, Y. Hoshi, Y. Kishimoto and N. Usami, *Opt. Express*, 2014, **22**, A225.
10 E. L. Warren, J. R. McKone, H. A. Atwater, H. B. Gray and N. S. Lewis, *Energy Environ. Sci.*, 2012, **5**, 9653.
11 S. Haussener, C. Xiang, J. M. Spurgeon, S. Ardo, N. S. Lewis and A. Z. Weber, *Energy Environ. Sci.*, 2012, **5**, 9922–9935.
12 S. M. Sze and K. K. Ng, *Physics of Semiconductor Devices*, Wiley-Interscience, 3rd edn, 2006.
13 S. M. Eichfeld, H. Shen, C. M. Eichfeld, S. E. Mohney, E. C. Dickey and J. M. Redwing, *J. Mater. Res.*, 2011, **26**, 2207–2214.
14 E. L. Warren, H. A. Atwater and N. S. Lewis, *J. Phys. Chem. C*, 2014, **118**, 747–759.
15 M. D. Kelzenberg, S. W. Boettcher, J. A. Petykiewicz, D. B. Turner-Evans, M. C. Putnam, E. L. Warren, J. M. Spurgeon, R. M. Briggs, N. S. Lewis and H. A. Atwater, *Nat. Mater.*, 2010, **9**, 239–244.